

A New Enhanced Microstrip Patch Antenna with Circular Polarization for mobile applications

Abdelilah AIT LAHCEN^{1*}, Samira CHABAA², Saida IBNYAICH¹, and Abdelouhab ZEROUAL¹

¹Department of Physics, I2SP Research Team, Faculty of Sciences Semlalia, Cadi Ayyad University, Marrakesh, Morocco

²Industrial Engineering Department, LISAD Research Laboratory National School of Applied Sciences, University Ibn Zohr, Agadir, Morocco

Abstract. This study shows an enhanced octagonal circularly polarized (CP) patch antenna, This one appropriate for mobile applications, such as wireless applications, especially for WIMAX, and 5G mid-band. A single-port excitation approach is utilized to obtain the intended outcome. The substrate used is Rogers RT/duroid 5880 with a relative permittivity of 2.2 and a low loss tangent (0.0009). The antenna's dimensions are optimized with the final design measuring $32 \times 35 \times 1.67$ mm³. To generate the circular polarization a square slot is cut, and two stubs are inserted in the opposite corners of the ground plane. A good result is achieved, for the reflection coefficient, we have a bandwidth (< -10 dB) of 1.29 GHz (2.8 GHz–4.09 GHz) and the bandwidth of the Axial ratio (AR) below 3 dB is 500 MHz (3.33 GHz–3.83 GHz). (CST) and (HFSS) softwares were used to calculate all obtained results. This microstrip antenna has a tiny dimension, it is simple to fabricate and has a lightweight, it has high performance, such as a wide band of the reflection coefficient of 1.29 GHz, also, its circular polarization makes it ideal for mobile applications, particularly WIMAX and 5G mid-band.

1 INTRODUCTION

Over the past several years, microstrip patch antennas have been the subject of substantial research, design, and use in a variety of wireless communication applications, such as satellite, mobile phone, weather radar, RFID applications, and remote sensing [1] [2] [3] [4] [5]. Because of their small size, light weight, affordability, and easy feeding methods, patch antennas are becoming more and more common. In particular, circularly polarized patch antennas are preferred in many applications due to their many advantages over linearly polarized ones, including better weather penetration, higher mobility, and better alignment between the transmitter and receiver.

A wide range of antennas have been created for wireless applications. In the last few years, circularly polarized printed antennas became the focus of numerous research articles. The study [6] proposes a wide-angle scanning circularly polarized shared-aperture array. Four bent metal pins and a metal cavity are added to enhance the wide-angle scanning capability. Consequently, the radiation pattern may be reshaped by inducing the parasitic current with the vertical component. The study [5] provides a high gain, high front-to-back ratio, small dimension, and high-performance metasurface (MS) based CP antenna. A 2×2 unit-cell MS is used in the suggested design to achieve its small size, and a coupling between the MS and a Y-shaped patch, which serves as the principal CP

source, realizes the CP. In paper [7] The microstrip antenna is designed to function in many bands, such as the mm-wave frequency bands of 40–60 GHz and 25–32 GHz. Wireless applications, especially those using 5G technology, are affected by these frequency bands. In [8] suggests a microstrip patch antenna with a diagonal form and circular polarization for mobile and Wi-Fi applications. The radiating patch resonates at 2.64 GHz with circular polarization and is sliced diagonally from opposite corners. The study [9] presents a method for producing circular polarization (CP) with just one radiator. By utilizing the functioning processes of traditional sequentially-rotated radiator antennas, the sequentially-rotated feeding network was able to provide comparable CP performance without compromising compact size.

In this paper a wide-band circularly polarized antenna with a simple design that achieves by increasing the bandwidth at 3-dB of the axial ratio using a square slot and parasitic element in the ground plane. The antenna is built on a single substrate layer using a Rogers RT/duroid 5880 substrate with a 2.2 relative permittivity, a low loss tangent (0.0009), and fed via a 50 Ω microstrip line. It uses an octagonal patch as its primary radiating element. It is designed for WIMAX and 5G mid-band applications, covering a frequency range from 2.8 GHz to 4.09 GHz, it is circularly polarized in the band frequencies of 3.33–3.83 GHz.

The structure of this paper is as follow: Section 2 provides details on the suggested patch antenna design.

* Corresponding author: abdelilahaitlahcen4@gmail.com

To determine the ideal antenna design, Section 3 offers a parametric study. Section 4 outlines the procedure for validating the suggested antenna. The performance evaluation of the suggested antenna is shown in Section 5. Lastly, the significant findings of this paper are concluded in Section 6.

2 Design of the circularly polarized patch antenna

2.1 The suggested circularly polarized antenna

Fig. 1 shows the front, back, and side views of the suggested antenna. The antenna geometry for the recommended circularly polarized patch antenna is illustrated in Fig. 2. This antenna is printed on the Rogers RT/duroid 5880 dielectric at 1.6 mm thickness, with a loss tangent of 0.0009 and a relative permittivity ϵ_r of 2.2. The antenna has a square slot, two stubs, and

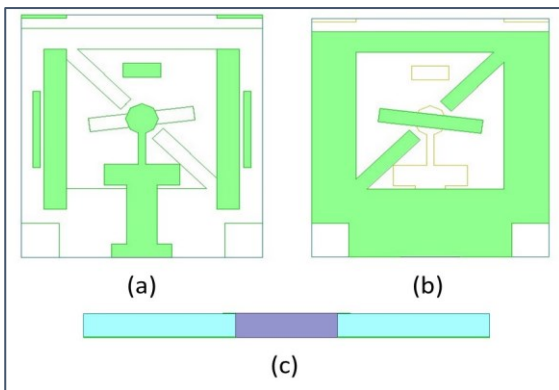


Fig. 1. Design of the suggested antenna (a) front view, (b) back view and (c) side view.

an parasitic element in the ground plane at the bottom surface, and a resonating element with an octagonal shape is printed on the top surface.

We use copper for the conductor elements (ground plane and resonating element). The antenna measures $32 \times 35 \times 1.67 \text{ mm}^3$ and is powered by a 50Ω microstrip line feed.

The table 1 presents the values of antenna parameters.

Table 1. Table of parameters and values

Parameters	Values(mm)	Parameters	Values(mm)
L1	33	W5	5
L2	20	W6	2
L3	5	W7	8.5
L4	8	W8	3
L5	5	W9	5.3
L6	10	W10	2
L7	5	W11	23
L8	3	W12	0.5
L9	1	W13	11
L10	6	M1	14
L11	15	M2	6
W1	35	D1	2
W2	32	D2	2
W3	20	R	2.2
W4	10	ϕ	7°

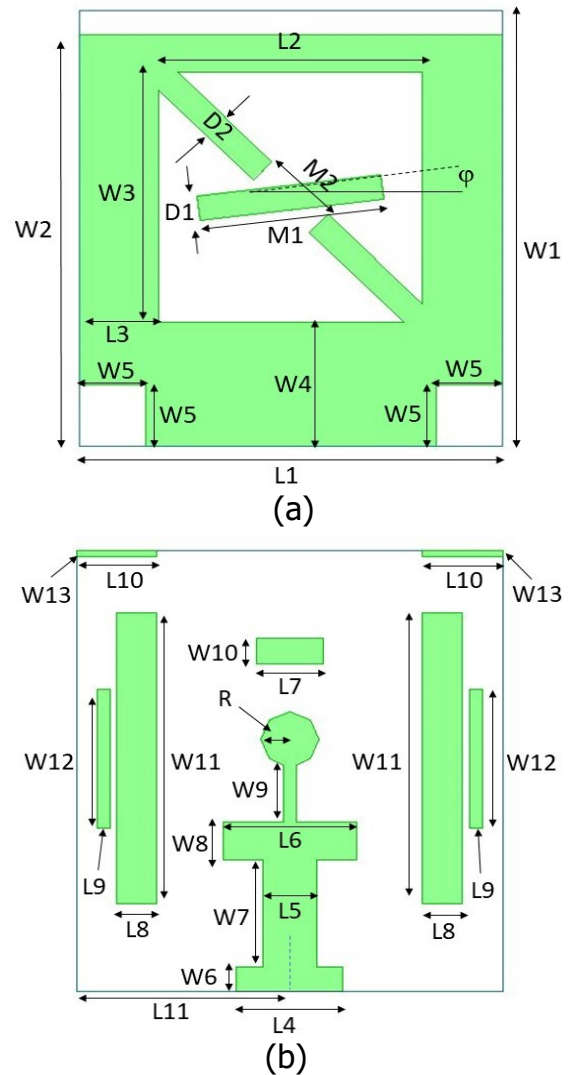


Fig. 2. The parameters of the antenna (a) ground plane (b) resonating element.

2.2 The process steps of the proposed antenna

The geometry of the suggested circularly polarized antenna with an octagon patch, firstly, antenna 1 is a patch antenna with an octagonal shape and a slot in the ground plane, as illustrates in Fig. 3.a, it is resonated at frequency of 3.5 GHz.

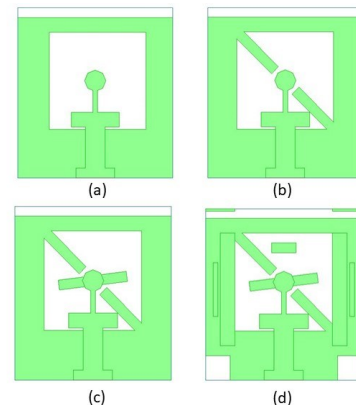


Fig. 3. Antenna evolution (a) Antenna 1, (b) Antenna 2, (c) Antenna 3, and (d) Antenna 4.

Two stubs are added in two corners opposite of the square to create a circular polarization (antenna 2) as shown in Fig. 3.b. We insert a rectangular parasitic element in the center of the slot for adjusting the resonant frequency of the axial ratio, (antenna 3), as presented in Fig. 3.c. For antenna 4, as shown in Fig. 3.d, we add a parasitic elements on the same side as resonant element and two square slots in the corners of the ground plane to increase the performance of this antenna.

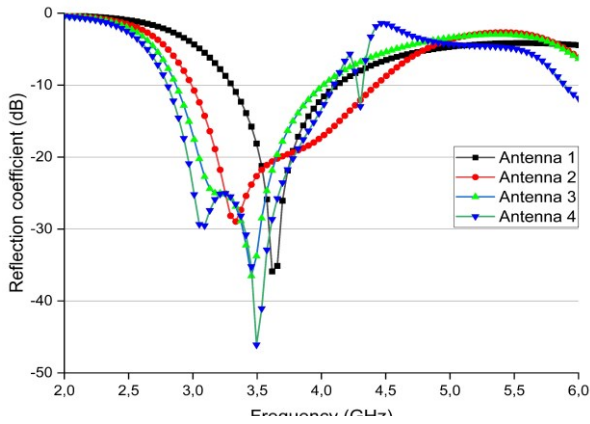


Fig. 4. The simulated reflection coefficient for the different steps of the proposed antenna (Antenna 1, Antenna 2, Antenna 3, and Antenna 4)

The obtained reflection coefficient of the different steps of the antenna is illustrated in Fig. 4, for this figure, we note that, for antenna 1, the resonant frequency is 3.62 GHz and the bandwidth is from 3.3 GHz to 4.11 GHz, and for antenna 2, the resonant frequency is 3.33 GHz and the bandwidth is from 2.98 GHz to 4.42 GHz, while for antenna 3, the resonant frequency is 3.45 GHz and the bandwidth is from 2.86 GHz to 4.01 GHz, the antenna 4 resonates at 3.5 GHz and the bandwidth is 1.29 (2.8 GHz-4.09 GHz).

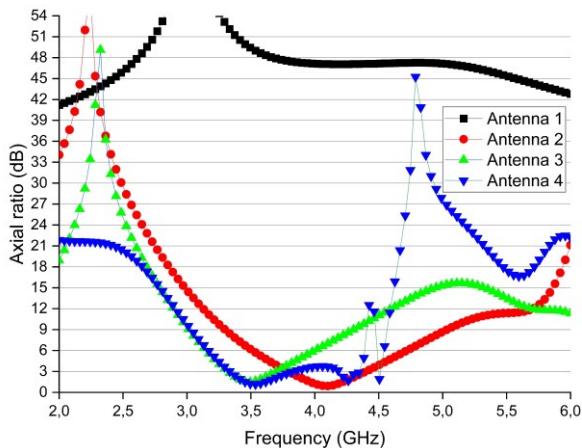


Fig. 5. The simulated axial ratio for the different steps of the proposed antenna (Antenna 1, Antenna 2, Antenna 3, and Antenna 4)

Fig. 5 illustrates the axial ratio of the different steps of the antenna, from antenna 1 to antenna 4. In this figure, we note that for antenna 1, the axial ratio is more than 3 dB in all the frequency bands, so it is not a circularly

polarized antenna. By adding the stubs in antenna 2, we obtain a circular polarization as illustrated in the figure; we obtain an axial ratio below 3 dB from 3.78 GHz to 4.39 GHz; but the desired frequency not covered, once adding the parasitic element in the center of the slot, the bandwidth of the axial ratio is enhanced; we obtain the circular polarization at the desired frequency with a bandwidth of 377 MHz (3.31 GHz-3.69 GHz), for antenna 4, The bandwidth is enhanced, it becomes 500 MHz (3.33 GHz-3.83 GHz).

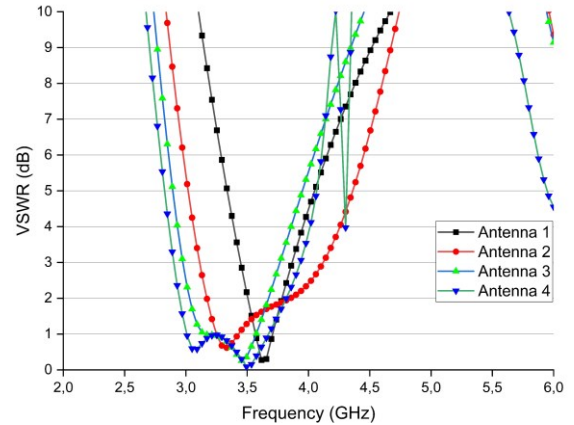


Fig. 6. The simulated voltage standing wave ratio for the different steps of the proposed antenna (Antenna 1, Antenna 2, Antenna 3, and Antenna 4).

Fig. 6 represents the voltage standing wave ratio (VSWR) of the four steps of the evolution of the antenna, Table 2 illustrates the VSWR bandwidth below 2 dB of the four antennas.

Table 2. The VSWR of the different steps of the antenna (from Antenna 1 to Antenna 4)

Evolution of the antenna	Ant 1	Ant 2	Ant 3	Ant 4
VSWR bandwidth (GHz)	3.5-3.78	3.17-3.89	3.02-3.67	2.94-3.83

From the obtained results, we can conclude that the obtained antenna can cover the totality of the WIMAX and 5G mid-frequency bands.

3 PARAMETRIC STUDY

Several parameters were adjusted during the optimization process. In the studies below, we will present the most important of them, we examine the effects of the radius of the octagon, and the dimensions of the parasitic element. The results are presented in the following sections:

3.1 The effect of the octagonal radius

The performance of the suggested antenna is affected by changing the radius (R) of the octagon.

For R = 1.6 mm, the bandwidth of the reflection coefficient is 1.19 GHz (3.3 GHz-4.27 GHz), including the desired frequency; this is illustrated in Fig. 7, and the circular polarization is obtained as shown in Fig. 8, its bandwidth is 236 MHz (3.38 GHz-3.61 GHz), we modify the radius, for R = 2.2 mm, the antenna resonates at the frequency of 3.5 GHz, covering a bandwidth from

2.8GHz to 4.09 GHz (1.29 GHz), and the reflection coefficient at 3.5 GHz is -44.98 Db. The circular polarization is achieved at the frequency of 3.5 GHz with a bandwidth of 3.33 GHz to 3.83 GHz (500 MHz). To optimize the characteristics of this antenna, we increase the value of the radius by 0.4 mm to become $R = 2.8$ mm. The results demonstrate a decrease in the characteristics of the antenna; exactly the reflection coefficient at 3.5 GHz becomes -17.5 dB. On the other hand, for $R = 2.2$ mm, it is equal to -44.98 dB.

We choose the radius of the octagonal radiating

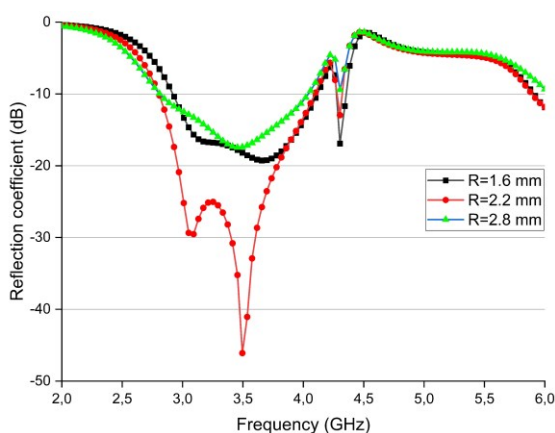


Fig 7. The reflection coefficient for different values of radius of octagon.

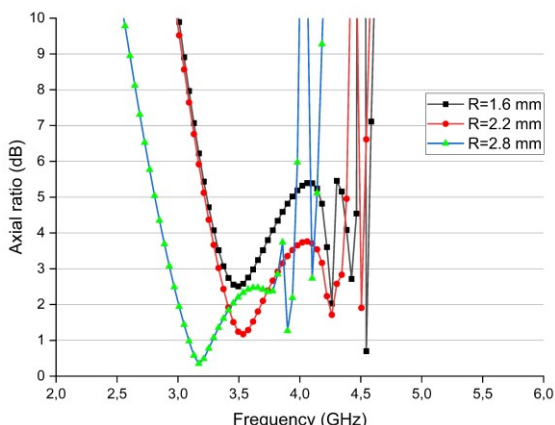


Fig. 8. The axial ratio for different values of radius of octagon.

element of $R = 2.2$ mm because, with this radius, we obtain the best results.

3.2 The effect of height and width of the parasitic element

The performance of the proposed antenna can be adjusted by modifying the parasitic element size.

For $M1=12$ mm and $D1=1.6$ mm, the reflection coefficient's bandwidth is from 2.82 GHz to 4.03 GHz, as demonstrated in Fig. 9, including the appropriate frequency. Also, the bandwidth of the axial ratio is from 3.4 GHz to 4.18 GHz, but does not centered at the frequency of 3.5 GHz, this is presented in Fig. 10.

To maximize the properties of this antenna, we modify the length and width to $M1=14$ mm and $D1=2$ mm. At this setting, the antenna nearly resonates at 3.5

GHz covering the bandwidth from 2.8 GHz to 4.09 GHz (1.29 GHz), and the circular polarization is obtained, the axial ratio cover the bandwidth from 3.33 GHz to 3.83 GHz (500 MHz). For more optimization, we increase the size to $M1=16$ and $D1=2.4$ mm. The antenna operates at frequency of 3.5 GHz, However, the bandwidth of the axial ratio decreases covering the bandwidth from 3.22 GHz to 3.51 GHz (289 MHz).

The optimal performance of the antenna is obtained with a size of $M1 = 14$ mm and $D1 = 2$ mm.

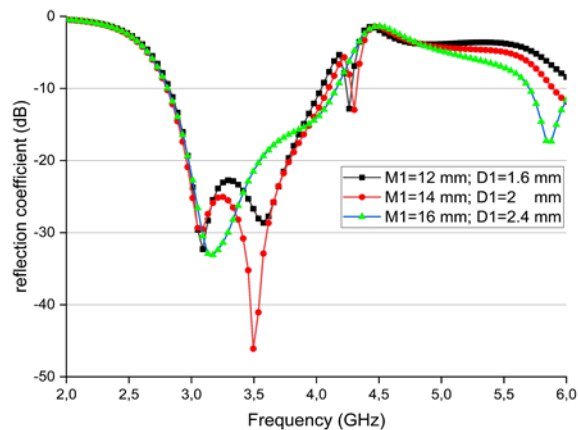


Fig. 9. The reflection coefficient for different values of $M1$ and $D1$.

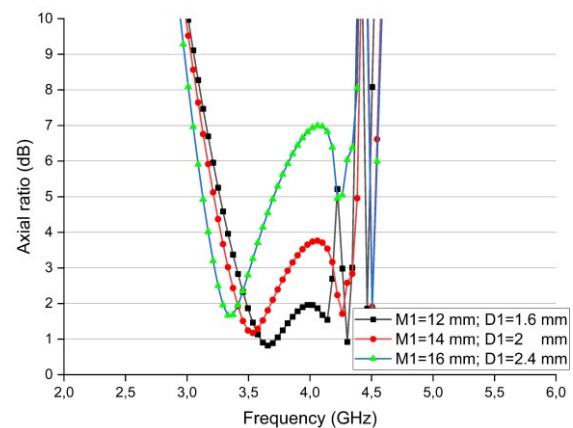


Fig. 10. The axial ratio for different values of $M1$ and $D1$.

4 VALIDATION OF THE OBTAINED RESULTS:

As illustrated in Fig. 11 the proposed antenna was designed and simulated also with the microwave studio CST software to validate the obtained results by the HFSS software, knowing that the two softwares use different methods, CST studio use the finite element method (FEM), the finite integration technique (FIT), and the transmission line matrix method (TLM), whereas HFSS is based on the finite element method (FEM).

One can remark that the reflection coefficient bandwidth obtained using HFSS is 2.8-4.09 GHz, the one achieved by CST is from 2.76 GHz to 4.18 GHz. The bandwidth of the axial ratio below 3 dB obtained by utilizing HFSS and CST, respectively, are from 3.33 GHz to 3.83 GHz and from 3.17GHz to 3.79 GHz, this is illustrated in Fig. 12. The both include the desired

frequency of 3.5 GHz, and cover the similar bandwidth, we note that the obtained results by HFSS are validated using CST software.

5 COMPARISON OF THE SUGGESTED

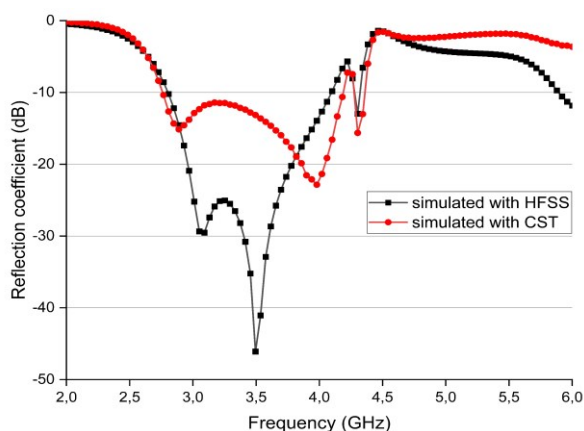


Fig. 11. The reflection coefficient simulated by HFSS and CST softwares.

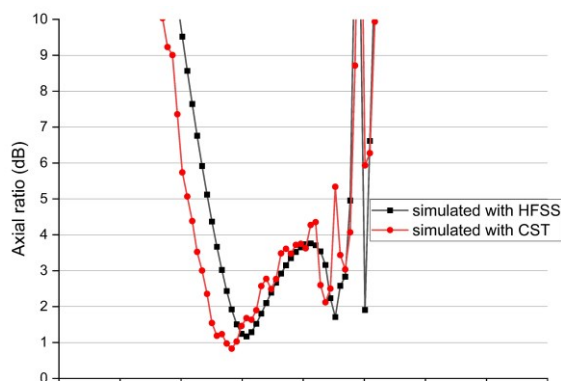


Fig. 12. The axial ratio simulated by HFSS and CST softwares.

CIRCULARLY POLARIZED PATCH ANTENNA WITH CORRESPONDING WORKS

To prove the effectiveness of our antenna, we draw a comparative table to compare the performance of our antenna compared to existing antennas in the literature, namely the size, the resonance frequency (f_0), the bandwidth of the reflection coefficient (S11(BW)), and the axial ratio bandwidth (AR(BW)).

Our antenna is optimized to cover the desired frequency and improved to operate in a bandwidth from 2.8 GHz to 4.09 GHz which is wider than in previous articles as shown in Table 3 except [12]. Also, the bandwidth of the axial ratio covers 3.33 GHz to 3.83 GHz (13.96 %) is large compared to those obtained in all studies except [12], but our antenna is more compact than antenna [12].

Table 3.Comparative study with recent antennas.

Ref.	Dimensions (mm ³)	f_0 (GHz)	S11 BW (%)	AR BW (%)
[10]	-	4.9/ 5.5	4.9/6.5	1.04/ 1.07

[11]	30*30*1.6	5.8	11.1	3.8
[6]	120*120*18.52	2.1/ 2.49	-	10.5/ 2.8
[12]	50 *5.25	7.6	-	14.7
[13]	50*50*0.8	5.8	7.6	<1
[14]	25*25	2.45/ 5.8	10.26/ 9.05	4.1/ 1.8
[15]	71*52*11.56	5.2	-	2.5
[16]	50*50*0.8	4.53/ 6.91	22.96/ 19.55	8.81/ 3.45
This work	32*35*1.6	3.5	37.44	13.96

6 Conclusion

A miniature octagonal microstrip antenna is excited by microstrip line has been developed to provide the WiMAX and 5G mid-band frequency band centered at 3.5 GHz. It has been observed that the resonant frequency of the antenna can be easily achieved. The impedance bandwidth is successfully controlled by utilizing a square slot. The circular polarization is generated by adding the rectangular stubs in two opposite corners on the diagonal of the square. we insert the rectangular parasitic element to shift the bandwidth of the axial ratio to cover the desired frequency. The antenna is compact in size, easy to construct, and has good performance. It is also suitable for mobile applications due to its circular polarization, which is especially suitable for WIMAX and 5G mid-band frequencies. Due to this characteristic, we are able to make it wherever we want, regardless of the location.

References

1. Y. Yuan, M. Li, G. Zhu, X. Qu, and Z. Li, “A Low Profile Wideband Circularly Polarized Patch Antenna Using Metasurface,” *Progress In Electromagnetics Research C*, vol. 144, pp. 55–64, (2024)
2. V. A. P. Chavali, A. A. Deshmukh, A. G. Ambekar, H. Vasudevan, and T. V. Sawant, “Reconfigurable Designs of Sectoral Microstrip Antennas for Wideband and Circularly Polarized Response,” *Progress In Electromagnetics Research C*, vol. 143, pp. 23–33, (2024)
3. B. Zeng and H. Zhu, “Designing a Dual-Feed Circular Polarization Antenna,” *Journal of Electronic Research and Application*, vol. 8, no. 3, (2024) <http://ojs.bbwpublisher.com/index.php/JERA>
4. R. Ruliyanta, R. Nugroho, and D. Asyifa, “Design of Rectangular Patch Array 2x4 Microstrip Antenna on C-Band for Weather Radar Applications,” *Journal of Telecommunication, Electronic and Computer Engineering (JTEC)*, vol. 16, no. 1, pp. 7–11, Mar. (2024)
5. H. Tran-Huy, H. H. Nguyen, and T. Hoang Thi Phuong, “A compact metasurface-based circularly polarized antenna with high gain and high front-to-back ratio for RFID readers,” *PLoS One*, vol. 18, no. 8 August, Aug. (2023)

6. L. Zhang, F. Lin, H. J. Sun, and J. Y. Yin, "A Wide-Angle Scanning Circularly Polarized Shared Aperture Array with Low Scan Loss Capability," *IEEE Antennas Wirel Propag Lett*, (2024)
7. H. El-Hakim and H. A. Mohamed, "Synthesis of a Multiband Microstrip Patch Antenna for 5G Wireless Communications," *J Infrared Millim Terahertz Waves*, vol. 44, no. 9–10, pp. 752–768, Oct. (2023)
8. S. Bhatia and M. V. Deepak Nair, "Single Feed Corner Trimmed Circularly Polarized Diagonal Patch Antenna," in *Lecture Notes in Electrical Engineering*, Springer, pp. 371–376, (2020)
9. L. M. Bieber, L. Wang, and W. Li, "A Single Radiator-Based Circularly Polarized Antenna for Indoor Wireless Communication Applications," *IEEE Open Access Journal of Power and Energy*, vol. 7, no. 1, pp. 111–121, (2020)
10. V. L. Pham, S. X. Ta, K. K. Nguyen, C. Dao-Ngoc, and N. Nguyen-Trong, "Single-Layer, Dual-Band, Circularly Polarized, Proximity-Fed Meshed Patch Antenna," *IEEE Access*, vol. 10, pp. 94560–94567, (2022)
11. M. R. Kattiakara Muni Samy and A. Gudipalli, "Design circular polarized antenna at ISM band for WBAN using parasitic elements," *Heliyon*, vol. 10, no. 6, Mar. (2024)
12. S. Genovesi and F. A. Dicandia, "Characteristic Modes Analysis of a Near-Field Polarization-Conversion Metasurface for the Design of a Wideband Circularly Polarized X-Band Antenna," *IEEE Access*, vol. 10, pp. 88932–88940, (2022)
13. H. W. Htun, E. Nishiyama, and I. Toyoda, "An Electrically Reconfigurable Circularly-Polarized Planar Array Antenna With Built-In Bias-Isolation Mechanism," *IEEE Access*, vol. 11, pp. 108317–108327, (2023)
14. C. Bajaj, D. K. Upadhyay, S. Kumar, and B. K. Kanaujia, "Directional Energy-Efficient Metasurface-Backed RFID Reader Antenna for Minimizing Tag-Detection Uncertainty in IoT Networks," *IEEE Journal of Radio Frequency Identification*, vol. 8, pp. 88–97, (2024)
15. P. Mondal, D. Dhara, and A. R. Harish, "A Partially Reflective FSS-Based Superstrate as a Decoupling Structure for Reducing the Mutual Coupling of Circularly Polarized Antennas," *IEEE Trans Antennas Propag*, vol. 72, no. 4, pp. 3652–3661, Apr. (2024)
16. A. R. Hossain, M. S. I. Sagar, A. A. Mertvy, P. K. Sekhar, and T. Karacolak, "Inkjet Printed Flexible Dual-Band Dual-Sense Circularly Polarized Patch Antenna," *IEEE Access*, vol. 12, pp. 55424–55433, (2024)